# Performance Assessment of PMU-Based Estimation Methods of Thevenin Equivalents for Real-Time Voltage Stability Monitoring

Jan Lavenius*, Luigi Vanfretti*†, Glauco N. Taranto‡
* Department of Electric Power Systems , KTH Royal Institute of Technology, Stockholm, Sweden
† Research and Development Division, Statnett SF, Oslo, Norway
‡ Department of Electrical Engineering, Federal University of Rio de Janeiro, Rio de Janeiro, Brazil.

***Abstract*—This paper investigates the performance of different methods for calculating the Thevenin equivalent parameters based using only data obtained from real-time synchrophasor measurements. Estimating the parameters from data affected by noisy measurements, transients, and continuously varying power system parameters may yield Thevenin equivalents that do not reflect the actual voltage stability of the system. The paper proposes using a total least squares method to take into account errors in the model from time-varying Thevenin parameters and noise. The paper reviews two different methods for Thevenin equivalent estimation proposed in the literature. The suitability of the three methods described in the paper is tested in case studies, where the performance of the methods are tested with both noise-free and noisy data. The papers also investigates effect of changes in the power consumptions at other buses on the Thevenin parameters seen from the monitored load bus.**

***Index Terms*—Least squares approximations, Synchrophasor applications, Voltage instability detection, Wide Area Monitoring Systems**

## I. Introduction

### A. Motivation

The operation of power systems of today is being transformed, due to increasing amounts of intermittent and distributed power stemming from the expansion of renewables, and by a more intense utilization of the existing grids. Tackling the changing patterns of the power flow through the transmission grid requires fast and accurate supervision and control, in order to predict and maintain the stability of the system [1]. Voltage stability is the system's capability of keeping the voltages in buses close to their nominal values after a disturbance. Failure to do so may negatively affect the delivery of power for large parts of the system, by forcing the disconnection of generators and loads.

Several different methods has been proposed in order to determine the maximum power that can be transmitted to load buses. These methods include coupled-port models, Thevenin equivalents and Ward-type equivalents. Reference [2] introduces the concept of coupled single-port models in order to take into account the effect of a simultaneous load increase at multiple loads. Reference [3] developed a method to calculate the Thevenin equivalent from terminal measurements based on Tellegen's theorem. In reference [4], the authors present an adaptive method for estimating Thevenin equivalent parameters. Reference [5] investigated the aforementioned methods and found that only two of the methods were appropriate for the specific system and contingencies that were considered. In [6], a method estimating the Thevenin equivalent recursive using constrained least square method is presented. For some PMU-based applications some of these methods may be unsatisfactory due to either the limited availability of PMU data in the system, or for their sensitivity to noise, or for their dependence on knowing the system configuration at all times.

This work was financially supported in part by *STINT* and *CAPES* through the program *Joint Brazilian-Swedish Research Collaboration*, by *Statnett SF* – the Norwegian power system operator, and by the *STandUP for Energy Collaboration Initiative*.

### B. Contributions

The paper proposes a Thevenin estimation algorithm based on the Total Least Squares (TLS) method and compares it against two other methods from literature that also use local PMU measurements. The performance of the Thevenin parameter estimation methods are evaluated based on their ability to correctly classify the voltage stability before and after a contingency. Correctly identified Thevenin equivalents can be used to track the maximum loadability of monitored load buses. This paper complements the evaluation of Thevenin equivalent estimation methods in [5], by shifting the scope to power systems subjected to contingencies and by considering noisy measurements. Case studies are performed by simulating the dynamic response of a power system which contains On-Load Tap Changers (OLTCs) and Over-Excitation Limiters (OELs) after being subjected to severe contingencies. In these case studies, the paper investigates the robustness of the methods, their over-all performance during the pre- and post-contingency state, and the impact of measurement noise.

978-1-4799-7993-6/15/$31.00 ©2015 IEEE

## II. Background

### A. PV-curves

Consider a load that consumes the complex power $\bar{S} = P + jQ$, which is provided from an ideal voltage source with a voltage magnitude of $V_1$ through a transmission line with resistance $R$ and reactance $X$. The following expression for the load bus voltage magnitude $V_2$ can be obtained

$$V_2^4+(2QX+2PR-V_1^2)V_2^2+(X^2+R^2)(P^2+Q^2)=0, \quad (1)$$

which is a quadratic equation with respect to $V_2^2$. By considering only real, positive solutions $V_1^2$ of (1) it is possible to express the voltage magnitude at the load bus as

$$V_2 = \sqrt{\frac{V_1^2}{2} - QX - PR \pm \frac{1}{2}\sqrt{D}}, \quad (2)$$

where $D$ is the discriminant given by

$$D = V_1^4 - 4\left((P+Q)(R+X)V_1^2 + 2PQRX\right). \quad (3)$$

By keeping the line impedance $\bar{Z} = R+jX$ and the voltage magnitude $V_2$ constant and smoothly increasing the complex power $\bar{S} = S\angle\phi$ consumed by the load, then for some $\bar{S}_{crit}$ the two distinct real solutions (2) will coalesce and vanish. This bifurcation point can be calculated by setting the discriminant $D$ of (3) to zero and solving for one of the variables. The complex power transferred at the bifurcation point will indicate the maximum transferable active power $P_{crit}$ to that load for a fixed $\phi$. When the load consumes $P_{crit}$, then the voltage will have dropped to $V_{crit}$, which is the voltage at which the two real voltage solutions of (2) coalesce.

### B. Thevenin equivalents

A Thevenin equivalent consists of a voltage source and an impedance that are series connected. This equivalent model can represent the terminal voltage and current of any one-port network. If the one-port network is non-linear or varies over time, then the Thevenin equivalent must be recalculated to accurately represent the terminal voltage and current for that specific time and operating point.

Consider the system shown in Fig. 1 where the load impedance $Z_{load}$ at Bus 2 consumes the complex power $P + jQ$. This power is supplied by an ideal voltage source $\bar{E}_{th}$ that is connected to the load by the impedance $Z_{th}$.

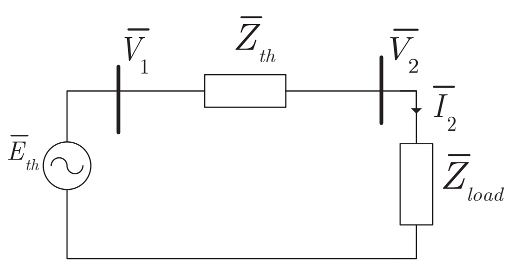


Fig. 1. Diagram of a load connected to a Thevenin equivalent.

It is possible to calculate the complex voltage $\bar{E}_{th}$ of the Thevenin equivalent in Fig. 1 from the voltage phasor $\bar{V}_2$ and the current phasor $\bar{I}_2$, if the impedance $\bar{Z}_{th}$ is known

$$\bar{E}_{th} - \bar{Z}_{th}\bar{I}_2 = \bar{V}_{load}. \quad (4)$$

Additionally, by measuring the current $\bar{I}_2$ and the voltage $\bar{V}_2$ at the load bus, the load impedance can be determined as $\bar{Z}_{load} = \bar{V}_2/\bar{I}_2$. The maximum power transfer theorem [7] states that the maximum power that can be transmitted to the load occurs when the apparent magnitudes of the line impedance and the load impedance match each other $Z_{load} = Z_{th}$. The difference in the magnitudes of the Thevenin impedance $Z_{th}$ and the load impedance $Z_{load}$ can therefore be used as a Voltage Stability Indicator (VSI).

## III. Existing Methods for estimating Thevenin equivalent Models

This section presents a short review of two existing methods for estimating the parameters of a Thevenin equivalent. These have in common that the system admittance matrix is not known and that only PMU measurements from a single bus are used.

### A. The Ordinary Least Squares (OLS) method

Separating the terms of (4) into real and imaginary parts, such that $\bar{I}_2 = I_r + jI_i$, $\bar{V}_2 = V_r + jV_i$, $Z_{th} = R_{th} + jX_{th}$ and $\bar{E}_{th} = E_r + jE_i$, give a linear system of equations

$$\boldsymbol{A}_k\boldsymbol{x} = \boldsymbol{b}_k = \begin{pmatrix} 1 & 0 & -I_r & I_i \\ 0 & 1 & -I_i & -I_r \end{pmatrix} \begin{pmatrix} E_r \\ E_i \\ R_{th} \\ X_{th} \end{pmatrix} = \begin{pmatrix} V_r \\ V_i \end{pmatrix}. \quad (5)$$

The system of equations in (5) contains four unknown variables in $\boldsymbol{x}$, i.e $E_r, E_i, R_{th}, X_{th}$, but the right hand side $\boldsymbol{b}_k$ has only two known variables, $V_r, V_i$ which means that (5) is an underdetermined system of equations. However, by taking measurements of $\bar{V}_2, \bar{I}_2$ at multiple time instances $k = 1, \ldots, M$ the following equation system is obtained

$$\mathbf{Ax} = \mathbf{b} \quad (6)$$

where $\mathbf{A} = [\mathbf{A}_1^T\, \mathbf{A}_2^T\, \ldots\, \mathbf{A}_M^T]^T$ and $\mathbf{b} = [\mathbf{b}_1^T\, \mathbf{b}_2^T\, \ldots\, \mathbf{b}_M^T]^T$. For $M = 2$, (6) will have a unique solution but typically the window length $M$ is chosen as $M \gg 2$ in order to filter out the impact of transients and noise. Therefore the system of equations in (6) will be overdetermined. A solution to (6) can be found by using the Ordinary Least Squares (OLS) method. The OLS seeks to minimize the Euclidean norm of the residuals, i.e. $\min \|\boldsymbol{Ax} - \boldsymbol{b}\|_2^2$ with respect to $\boldsymbol{x}$. This least squares problem has a simple closed form solution given by $\hat{\boldsymbol{x}} = (\boldsymbol{A}^T\boldsymbol{A})^{-1}\boldsymbol{A}^T\boldsymbol{b}$.

### B. Method using Tellegen's Theorem (TT)

Tellegen's theorem [3] in its difference form states that $\bar{\boldsymbol{I}}_{\boldsymbol{adj}}\Delta\bar{\boldsymbol{V}} - \bar{\boldsymbol{V}}_{\boldsymbol{adj}}^{\boldsymbol{T}}\Delta\bar{\boldsymbol{I}} = 0$ , where $\bar{\boldsymbol{I}}_{\boldsymbol{adj}}, \bar{\boldsymbol{V}}_{\boldsymbol{adj}}$ are the vectors of bus voltages and branch currents, respectively, of the adjoint system. In [3], the authors show that the difference form of Tellegen's theorem implies that the Thevenin impedance $\bar{Z}_{th}$

of the Thevenin equivalent connected to load, as shown in Fig. 1, can be estimated by

$$\bar{Z}_{th} = \frac{\Delta \bar{V}_2}{\Delta \bar{I}_2^*}. \tag{7}$$

In practice, when using (7) to estimate the Thevenin impedance, the difference $\Delta \bar{I}_2^*$ must be sufficiently large in order to avoid numerical problems [5]. Therefore (7) should only be evaluated when $|\Delta \bar{I}_2^*|$ is larger than a suitable threshold $\epsilon$. Hence, $Z_{th}$ will be held constant during some periods when there is little change in the current. During these times, the Thevenin voltage source $\bar{E}_{th}$ is calculated using (4).

## IV. The Total Least Squares (TLS) method

The proposed TLS method is similar to the classical OLS method; it also seeks to find the Thevenin parameters as a minimal solution to the equation system (6). It can be seen from (5) that the third and fourth column of $\boldsymbol{A}_k$ contain PMU data which may be noisy. The total least squares method takes into account that both the given matrix $\boldsymbol{A}$ and the given vector $\boldsymbol{b}$ of (6) may contain measurement errors. Therefore, the problem is to find a solution $\boldsymbol{x}$ to the corrected equation system $(\boldsymbol{A}+\Delta\boldsymbol{A})\boldsymbol{x} = (\boldsymbol{b}+\Delta\boldsymbol{b})$, or equivalently

$$\left(\boldsymbol{A} + \Delta\boldsymbol{A} \mid \boldsymbol{b} + \Delta\boldsymbol{b}\right) \begin{pmatrix} \boldsymbol{x} \\ -1 \end{pmatrix} = \boldsymbol{0}. \tag{8}$$

The corrections $\Delta\boldsymbol{A}$ and $\Delta\boldsymbol{b}$ in (8) are chosen such that they minimize the Frobenius norm of the correction matrix $(\Delta\boldsymbol{A} \mid \Delta\boldsymbol{b})$ while being subject to that the corrected system of equations (8) must hold, which gives the following minimization problem

$$\min_{(\Delta\boldsymbol{A}|\Delta\boldsymbol{b}),\boldsymbol{x}} \quad \|(\Delta\boldsymbol{A} \mid \Delta\boldsymbol{b})\|_F, \tag{9a}$$

$$s.t. \qquad (\boldsymbol{A} + \Delta\boldsymbol{A})\boldsymbol{x} \;= (\boldsymbol{b} + \Delta\boldsymbol{b}). \tag{9b}$$

The problem (9) can be solved using the Singular Value Decomposition (SVD) of the $m\times(n+1)$ matrix $(\boldsymbol{A} \mid \boldsymbol{b})$ [8]. The SVD of $(\boldsymbol{A} \mid \boldsymbol{b})$ is given by $\boldsymbol{U}\boldsymbol{\Sigma}\boldsymbol{V}^T$, where $\boldsymbol{V}$ is a $(n+1)\times(n+1)$ matrix with columns consisting of the right singular vectors to $(\boldsymbol{A} \mid \boldsymbol{b})$. The diagonal matrix $\boldsymbol{\Sigma}$ is of size $(n+1)\times(n+1)$ and has the singular values $\sigma_i, i = 1, \ldots, n+1$, of $(\boldsymbol{A} \mid \boldsymbol{b})$ on the diagonal. The singular values in $\boldsymbol{\Sigma}$ are assumed to be ordered with descending magnitude. If the singular value $\sigma_{n+1}$ is non-zero then equivalently the rank of $(\boldsymbol{A} \mid \boldsymbol{b})$ is $n+1$, which means that the system of equations is incompatible [9]. Therefore, the rank must be reduced to $n$. The best rank $n$ approximation $(\hat{\boldsymbol{A}} \mid \hat{\boldsymbol{b}})$ of $(\boldsymbol{A} \mid \boldsymbol{b})$ is given by the Eckhart-Young-Mirsky theorem [9] which states that

$$\min_{\text{rank}(\boldsymbol{A}+\Delta\boldsymbol{A}|\boldsymbol{b}+\Delta\boldsymbol{b})<n+1} \|(\Delta\boldsymbol{A} \mid \Delta\boldsymbol{b})\|_F = \sigma_{n+1} > 0. \tag{10}$$

What now remains is to find a solution $\hat{\boldsymbol{x}}$ such that the corrected equation system $\hat{\boldsymbol{A}}\hat{\boldsymbol{x}} = \hat{\boldsymbol{b}}$ holds. Partitioning of the SVD decomposition of $(\hat{\boldsymbol{A}} \mid \hat{\boldsymbol{b}})$ will give the following equation system:

$$(\hat{\boldsymbol{A}} \mid \hat{\boldsymbol{b}}) = \overset{\quad n \qquad 1}{\begin{pmatrix} \boldsymbol{U}_1 & \boldsymbol{U}_2 \end{pmatrix}} \overset{n \quad 1}{\begin{pmatrix} \boldsymbol{\Sigma}_1 & \boldsymbol{0} \\ \boldsymbol{0} & 0 \end{pmatrix}} \begin{matrix} n \\ 1 \end{matrix} \overset{n \qquad 1}{\begin{pmatrix} \boldsymbol{V}_{11}^T & \boldsymbol{V}_{21}^T \\ \boldsymbol{V}_{12}^T & V_{22}^T \end{pmatrix}} \begin{matrix} n \\ 1 \end{matrix}, \tag{11}$$

where the unitary matrices $\boldsymbol{U}, \boldsymbol{V}$ can be obtained from the SVD of $(\boldsymbol{A} \mid \boldsymbol{b})$. Using that the columns of the unitary matrix $\boldsymbol{V}$ in (11) are orthogonal to each-other it can be shown that $(\boldsymbol{V}_{12}^T \mid V_{22})^T$ is a right singular vector to $(\hat{\boldsymbol{A}} \mid \hat{\boldsymbol{b}})$, i.e. that

$$(\hat{\boldsymbol{A}} \mid \hat{\boldsymbol{b}}) \begin{pmatrix} \boldsymbol{V}_{12} \\ V_{22} \end{pmatrix} = 0 \tag{12}$$

holds. By substituting $(\boldsymbol{A}+\Delta\boldsymbol{A} \mid \boldsymbol{b}+\Delta\boldsymbol{b})$ with $(\hat{\boldsymbol{A}} \mid \hat{\boldsymbol{b}})$ in (8) and comparing the resulting equation with (12), a solution $\hat{\boldsymbol{x}}$ to $\hat{\boldsymbol{A}}\hat{\boldsymbol{x}} = \hat{\boldsymbol{b}}$ can be determined as

$$\hat{\boldsymbol{x}} = -\boldsymbol{V}_{12} V_{22}^{-1}. \tag{13}$$

If the scalar $V_{22}$ is non-zero then (13) is the solution the TLS problem and the TLS problem is called generic. If $\sigma_n > \sigma_{n+1}$ then this TLS solution is unique [10]. Methods to solve non-generic TLS problems also exists [9].

## V. Results

The proposed TLS Thevenin estimation described in Section IV was tested, together with the two methods described in Section III using data obtained from time-domain simulations. The methods were implemented as scripts the MATLAB environment. The phasor measurements were obtained by simulating the power systems in MATLAB using the Simulink-package, which is a tool for simulating dynamic systems.

The considered system is a small 5-bus model that is prone to voltage instability. The one-line diagram of the 5-bus system, adapted from [11], is shown in Fig. 2. The system contains a voltage dependent load at Bus 5 connected to Bus 4 through an OLTC controlling the voltage of Bus 5. The 5-bus system is connected to the rest of the grid at Bus 1. The bulk of the power consumed by the load is transmitted through the two parallel lines between Bus 1 and Bus 2. The generator located at Bus 2 is equipped with an automatic voltage regulator and an OEL.

The output of the methods were calculated by processing simulated phasor data $\bar{V}_4, \bar{I}_5$ sampled with a rate of 50 samples per second. The phasor $\bar{I}_5$ denotes the complex current drawn by the load at Bus 5 through the OLTC. To represent noisy data complex Additive White Gaussian Noise (AWGN) is added to each of the phasor measurements giving a Signal-to-Noise Ratio (SNR) of 110 dB. The window length of the OLS and the TLS methods was chosen to be $M = 1000$ samples.

Two contingencies were considered. In the first case, a tripped line causes the system voltage to degrade over time as a result of the tap changing of the OLTC, which is trying to restore the load voltage, and the activation of the OEL, which limit the field current $I_{field}$ of the generator. The second case, consists of the same line tripping, but now the parameters of the Grid Equivalent of Fig 2 are being varied to reflect changing power consumption of loads at that part of the grid.

### A. *Case 1: Disconnection of a line in the 5-bus system*

This case considers a contingency where one of the two parallel lines between Bus 2 and Bus 3 in Fig. 2 is tripped after 1 s of simulation. The resulting voltage magnitudes at

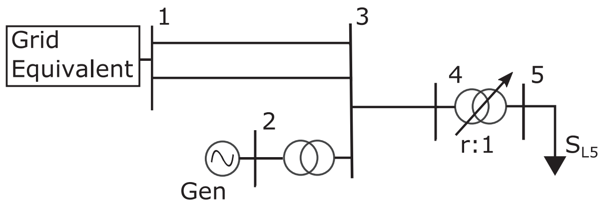


Fig. 2. Diagram of the 5-bus system.

Bus 4 and Bus 5 are shown in Fig. 3. From the figure it can be seen that the OLTC is unable to restore the voltage at Bus 5 to its nominal value and that after 61.1 s the tap-changing of the OLTC is no longer increasing the voltage at Bus 5l.

By plotting the voltage magnitude $V_4$ as a function of the active power $P$ that is consumed by the load, the PV-curve in Fig. 4 is obtained. From the PV-curve in Fig. 4 it can be seen

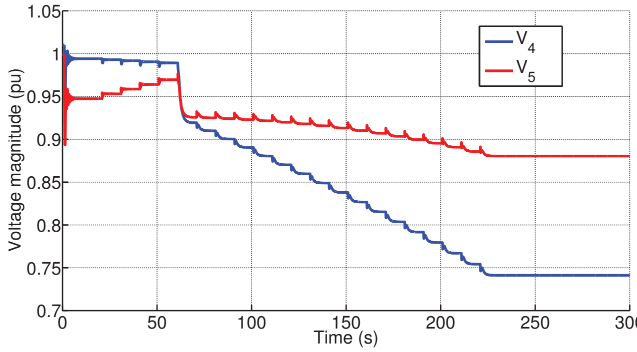


Fig. 3. The voltage magnitude of Bus 4 and Bus 5 in the 5-bus system for Case 1.

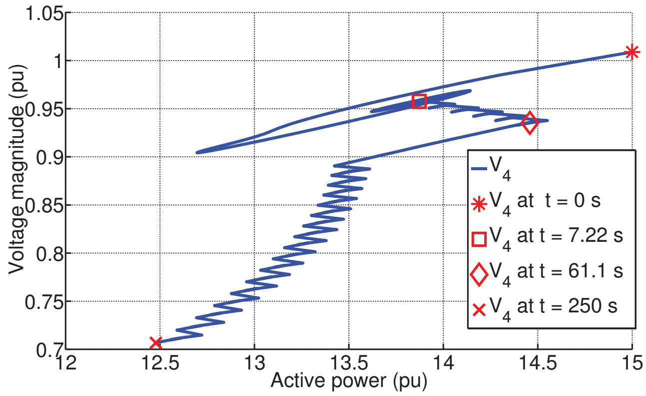


Fig. 4. The PV-curve of Bus 4 in the 5-bus system for Case 1.

that the transients of the line disconnection have disappeared after 7.21 s. Between 7.21 s and 61.1 s the evolution of the voltage $V_4$ and the consumed power $P_{L5}$ is driven by the OLTC between Bus 4 and Bus 5 which is regulating the voltage at Bus 5. During this period, the OLTC successfully increases the consumed power by changing the tap ratio, which indicates that operating point is on the upper part of the PV-curve, where the change in power consumed by the load and the change in voltage magnitude is not positively correlated. After 61.1 s the OEL of the generator at Bus 1 forces the field current back to its upper limit. After this time, the tap changes of the OLTC can no longer increase the power while lowering the bus voltage at Bus 4. Therefore, the operating points are on the lower part of the PV-curve at all times after 61.1 s, having bypassed the maximum power point. Next, the paper present the results obtained for Case 1 by the three different Thevenin equivalent estimation methods that were described in Sections III and IV.

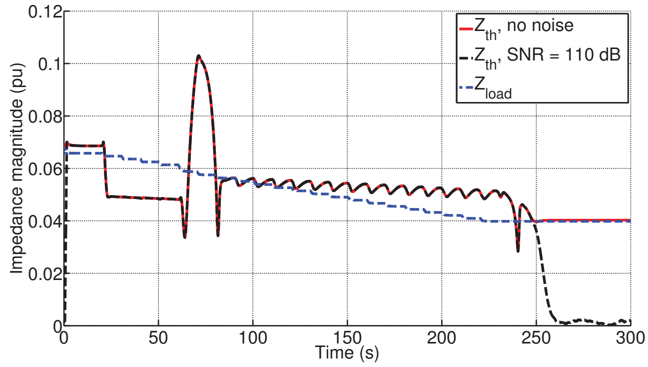


Fig. 5. Impedance magnitudes from the OLS method for Case 1.

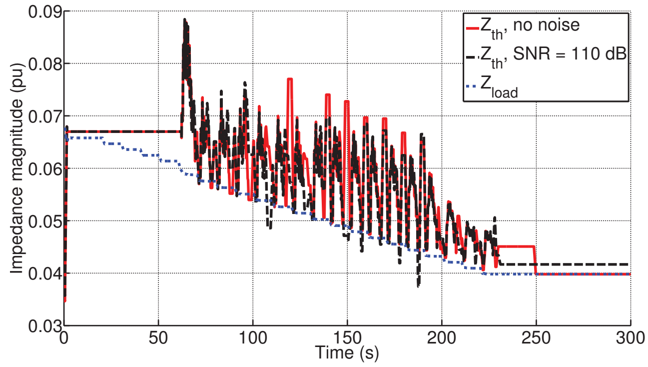


Fig. 6. Impedance magnitudes from the TT method for Case 1.

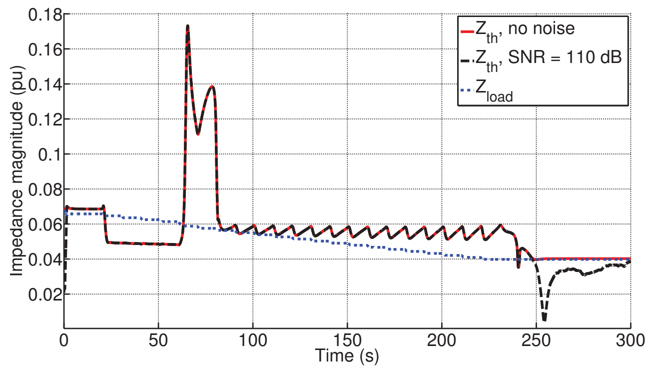


Fig. 7. Impedance magnitudes from the TLS method for Case 1.

In order to correctly classify the stability of the system, the crossing of the load impedance and the Thevenin impedance

$Z_{th} = Z_{load}$ should occur as soon as possible after 61.1 s. It is at this time the over-excitation limiter is activated, taking the system from an operation point on the upper part $V_4 > V_{crit}$ of one PV-curve of Bus 4, to the lower part $V_4 < V_{crit}$ of another without passing through the point of maximum power transmission $V_4 > V_{crit}$ of either PV-curve.

In Fig 5, the magnitudes of the load impedance and the Thevenin impedance as estimated by OLS are plotted. For the noise-free case the OLS provides good results before and after the OEL activation. For the noisy case, it can be seen that the measurements correctly indicate the voltage stability during the period when the load impedance is changing through OLTC actions. During the final seconds of the simulation, with no tap-changing, the method estimates that $Z_{th} < Z_{load}$, which wrongly suggests that the load bus voltage is on the upper part of the PV-curve. This result indicates that the OLS method is sensitive to noise.

The results for the TT method with a threshold $\epsilon = 10^{-3}$ are shown in Fig. 6. For both the noise-free and the noisy signals, the TT method is erroneously indicating that the system has passed the maximum power transfer point even before the OEL is activated. The TT method seems relatively unperturbed by the added measurement noise. except for an increase in the variability of the estimate.

In Fig. 7 the results of the TLS method are shown. The figure shows that the method gives similar or better results as the OLS method. The behavior of the algorithms after OEL activation is better, as there are fewer crossings between the impedances compared to the OLS method. Comparing the Figures 5-7, it can be seen that the TLS method is the method which are closest to identifying the true state of the voltage stability of the system during the period. The TT-method gives too conservative results before OEL activation and gives good results after OEL activation.

TABLE I
RESULTS FOR THE METHODS IN CASE 1.

| Method | Time used | Percent of samples estimating (in-)stability correctly | | | |
|---|---|---|---|---|---|
| | | Before OEL | | After OEL | |
| | | No noise | With Noise | No Noise | With Noise |
| OLS | 6.43 s | **65%** | **68%** | 89% | 68% |
| TT | **0.02 s** | 3% | 3% | 78% | 65% |
| TLS | 5.15 s | **65%** | 65% | **97%** | **84%** |

In Table I we summarize Case 1, by giving the time consumption of the methods and a quantitative indication of their performance during the evolution of the system instability, both with and without noise added to the measurements. Bold numbers are used to indicate that the corresponding method performed better than the other methods for that particular performance category. The OLS and TLS method give $Z_{th} < Z_{load}$ during a majority of the time for the period after the line disconnection and before the OEL activation. From the PV-curve, it can be seen that power consumption increases when the tap ratio is increased during this period suggesting that that the operating point is above $V_{crit}$ during this period. Therefore only OLS and TLS method that correctly identifies that the system has not passed the maximum power point before the OEL activation. From the first column of Table I, it can seen that the TLS and the OLS methods have similar computational costs and that the TT method is considerably faster. However, all methods are quite computationally cheap in terms of CPU-time considering that the simulation time is 300 seconds and that the data is sampled with a rate of 50 samples per second. All three methods would therefore be suitable to be implemented as real-time applications.

### *B. Case 2: Line disconnection and increased consumption in another load connected to the feeder*

The model considered in Case 2 is the same 5-bus system as in Case 1 except the Grid Equivalent in Fig. 2. This equivalent, representing the rest of grid, is now made variable. We model the Grid Equivalent as a radial feeder, with a variable shunt load is located in the middle of the feeder. The 5-bus system is considered to be connected to the end of this feeder. To simplify the calculations, the shunt load will be represented as a variable reactance $X_{sh}$ that is linearly decreased during the time span between 10 s and 125 s. The resulting impedance of the Grid Equivalent will then be non-linear and decreasing during this time span. Similar to Case 1, the maximum power consumption occurs when the OEL is activated. For Case 2 the OEL activation occurs after 60.8 s, thereafter subsequent tap changes of the OLTC between Bus 4 and Bus 5 will lead to both lowered voltage at Bus 4 and lowered power consumption $P_{L5}$.

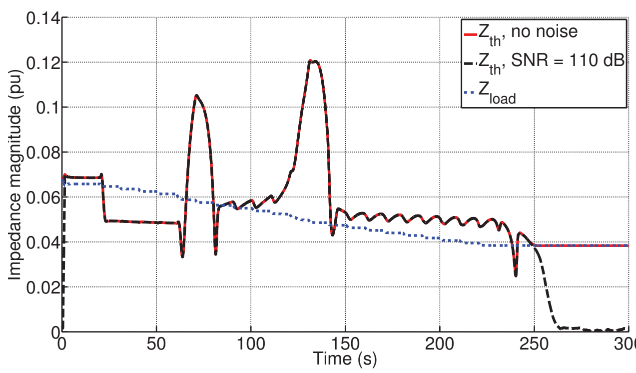


Fig. 8. Impedance magnitudes from the OLS method for Case 2.

In Fig. 8, the results of the OLS method is shown. The OLS method correctly identifies the voltage stability during most of time before the OEL is activated. After the OEL activation, the OLS method give acceptable results, until it reaches steady-state. At steady-state for the post-contingency system the noise has a large impact with an estimated Thevenin impedance $Z_{th} < Z_{load}$ for the noisy case, as was seen in Case 1.

The results from the TT-method in Case 2 are given in Fig. 9. The figure shows that the TT-method gives very conservative estimates of the stability of the system before the OEL activation. The impact of noise is very low for this case,

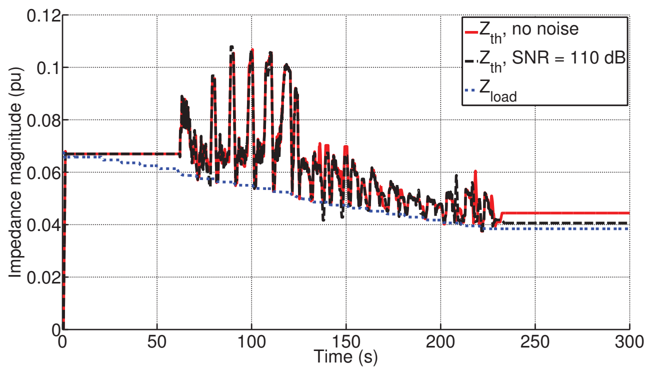


Fig. 9. Impedance magnitudes from the TT method for Case 2.

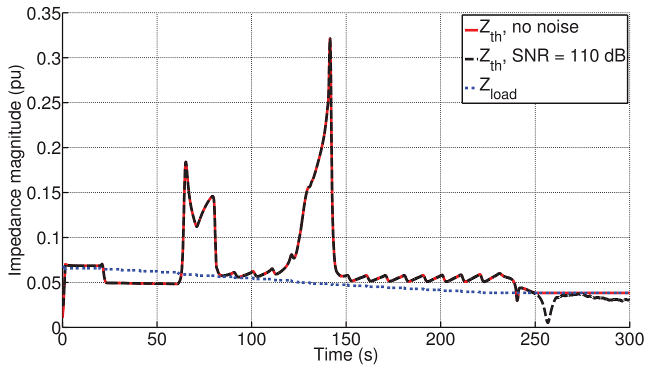


Fig. 10. Impedance magnitudes from the TLS method for Case 2.

which is evident in the steady-state of the post-contingency system. The low impact of the noise can be explained by the choice of a relatively high threshold $\epsilon$ so that the algorithm does not update the Thevenin estimate for small changes in the measured currents.

Finally, the results of the TLS method are given in Fig. 10. The results are very similar to Case 2, with a mainly correct identification of the stability of the system. The TLS method seems to be less sensitive than the OLS method to noise. The results for Case 2 are summarized in Table II.

TABLE II
RESULTS FOR THE METHODS IN CASE 2.

| Method | Percent of samples estimating (in-)stability correctly | | | |
|---|---|---|---|---|
| | Before OEL | | After OEL | |
| | No noise | With noise | No Noise | With noise |
| OLS | 66% | **68%** | 73% | 72% |
| TT | 3% | 3% | **100%** | **99%** |
| TLS | **68%** | **68%** | 78% | 77% |

## VI. DISCUSSION

This paper compared the performance of three methods used to estimate Thevenin equivalent parameter from PMU measurements obtained at a load bus. By correctly identifying the Thevenin parameters as seen from the load one can determine when the maximum loadability of a load is reached.

The proposed Total Least Squares method showed good performance in terms of classifying the voltage stability correctly for the combinations of the considered methods and cases. In comparison, the method based on Ordinary Least Squares displayed similar performance when the system was stable, and slightly worse performance when the system was unstable. The Total Least Squares method also showed a slightly reduced sensitivity to measurement noise compared to the Ordinary Least Squares method, which was most evident when there were no changes in the loading of the system. The window length used for these methods were quite long which may be a disadvantage when used as an input for taking corrective actions against voltage stability. The method based on Tellegen's Theorem showed good performance, but was very conservative when estimating the stability of the system before it passed the maximum loadability point.

Future work would include testing the methods for larger power systems and to compare the best performing sequential estimation algorithms with some of the recursive methods proposed in literature. To assess the suitability of these methods for being inputs to stabilizing to control in practical real-time implementations will require closed-loop testing, where the methods used for both stability assessment and stabilizing control are interfaced with to the power system, which can either be real or simulated [12]. Hardware-in-the-loop testing of PMUs will also more closely determine the impact of measurement noise on these methods.

## REFERENCES


[1] K. Moslehi and R. Kumar, "A reliability perspective of the smart grid," *Smart Grid, IEEE Transactions on*, vol. 1, no. 1, pp. 57–64, June 2010.

[2] Y. Wang, I. Pordanjani, W. Li, W. Xu, T. Chen, E. Vaahedi, and J. Gurney, "Voltage stability monitoring based on the concept of coupled single-port circuit," *Power Systems, IEEE Transactions on*, vol. 26, no. 4, pp. 2154–2163, Nov 2011.

[3] I. Smon, G. Verbic, and F. Gubina, "Local voltage-stability index using Tellegen's theorem," *Power Systems, IEEE Transactions on*, vol. 21, no. 3, pp. 1267–1275, Aug 2006.

[4] S. Corsi and G. Taranto, "A real-time voltage instability identification algorithm based on local phasor measurements," *Power Systems, IEEE Transactions on*, vol. 23, no. 3, pp. 1271–1279, Aug 2008.

[5] H. Yuan and F. Li, "A comparative study of measurement-based Thevenin equivalents identification methods," in *North American Power Symposium (NAPS), 2014*, Sept 2014, pp. 1–6.

[6] G. Fusco, A. Losi, and M. Russo, "Constrained least squares methods for parameter tracking of power system steady-state equivalent circuits," *Power Delivery, IEEE Transactions on*, vol. 15, no. 3, pp. 1073–1080, Jul 2000.

[7] T. Van Cutsem and C. Vournas, *Voltage Stability of Electric Power Systems*. Kluwer Academic Publisher, 1998.

[8] G. H. Golub and C. F. Van Loan, "An analysis of the total least squares problem," *SIAM Journal on Numerical Analysis*, vol. 17, no. 6, pp. 883–893, 1980.

[9] S. Van Huffel and J. Vandewalle, *The Total Least Squares Problem*. Society for Industrial and Applied Mathematics, 1991.

[10] I. Markovsky and S. V. Huffel, "Overview of total least-squares methods," *Signal Processing*, vol. 87, no. 10, pp. 2283 – 2302, 2007.

[11] M. Glavic and T. Van Cutsem, "Wide-area detection of voltage instability from synchronized phasor measurements. part I: principle," *IEEE Transactions on Power Systems*, vol. 24, pp. 1408 – 1416, 2009.

[12] R. Leelaruji and L. Vanfretti, "Detailed modelling, implementation and simulation of an 'all-in-one' stability test system including power system protective devices," *Simulation Modelling Practice and Theory, Elsevier,*, vol. 23, pp. 36–59, 2012.